



GLOBAL JOURNAL OF COMPUTER SCIENCE AND TECHNOLOGY: H
INFORMATION & TECHNOLOGY
Volume 16 Issue 3 Version 1.0 Year 2016
Type: Double Blind Peer Reviewed International Research Journal
Publisher: Global Journals Inc. (USA)
Online ISSN: 0975-4172 & Print ISSN: 0975-4350

Application of Computer Programming to Estimate Volumetric Change of an Active Drilling Fluid System Cause by Elastic Deformation of an Open Borehole Section Wall

By Asad Elmgerbi, Gerhard Thonhauser, Michael Prohaska, Abbas Roohi
& Andreas Nascimento

Montan University Leoben

Abstract- Volumetric changes in the active drilling fluid system during drilling operation are commonly termed borehole ballooning or breathing. One of the borehole ballooning contributors is the elastic deformation of an open borehole wall. When the elastic deformation of the open borehole wall occurs, it causes a volumetric change in the active drilling fluid volume in the system; the change in volume will be variable depending on the well in question and occurs frequently. Prediction of the volumetric change is highly complex, simply because huge number of complicated equations involved. Therefore, the use of the computer is necessary to reduce the process time and improve the prediction accuracy. Hence, Standalone software has been developed (built on Matlab) in order to estimate and quantify the volumetric change of the active drilling fluid system.

GJCST-H Classification: D.1.2 D.1.3



Strictly as per the compliance and regulations of:



© 2016. Asad Elmgerbi, Gerhard Thonhauser, Michael Prohaska, Abbas Roohi & Andreas Nascimento. This is a research/review paper, distributed under the terms of the Creative Commons Attribution-Noncommercial 3.0 Unported License <http://creativecommons.org/licenses/by-nc/3.0/>), permitting all non-commercial use, distribution, and reproduction in any medium, provided the original work is properly cited.

Application of Computer Programming to Estimate Volumetric Change of an Active Drilling Fluid System Cause by Elastic Deformation of an Open Borehole Section Wall

Asad Elmgerbi ^α, Gerhard Thonhauser ^σ, Michael Prohaska ^ρ, Andreas Nascimento [¥] & Abbas Roohi ^ω

Abstract- Volumetric changes in the active drilling fluid system during drilling operation are commonly termed borehole ballooning or breathing. One of the borehole ballooning contributors is the elastic deformation of an open borehole wall. When the elastic deformation of the open borehole wall occurs, it causes a volumetric change in the active drilling fluid volume in the system; the change in volume will be variable depending on the well in question and occurs frequently. Prediction of the volumetric change is highly complex, simply because huge number of complicated equations involved. Therefore, the use of the computer is necessary to reduce the process time and improve the prediction accuracy. Hence, Standalone software has been developed (built on Matlab) in order to estimate and quantify the volumetric change of the active drilling fluid system. The main objective of the presented Standalone software is to utilize the existing *in situ* principal stresses gradients, pore pressure gradient and rock geo-mechanical properties in order to compute the change in borehole volume for different flow rates. Moreover, it indicates any possible changes might occur to the equivalent circulating density within the referred system. The core of the presented Standalone software are two analytical formulas, which initially are used to estimate the radial elastic displacement for any point along the open borehole wall, which in turn will be utilized to quantify the volumetric change of the drilling fluid system for the entire open borehole section. The complete governing equations of the developed software are provided and described in detail. In order to examine the functionality of the software, two case studies have been performed using the developed software, several scenarios were assumed for both cases. The base scenario was defined to use the actual well data without any changes, whereas the changes have been

applied for the other scenarios. The main finding of these studies was that the volumetric change of the open borehole section, due to the elastic deformation of the open borehole wall, is not significant and mainly controlled by the pump flow rate, drilling fluid weight and temperature.

I. INTRODUCTION

Certainly, three processes can cause volumetric changes to the active drilling system, these process are:

- *Kick*: A flow of formation fluids into the wellbore during drilling operations.
- *Loss*: The leakage of the liquid phase of a drilling fluid, slurry or treatment fluid containing solid particles into the formation matrix.
- *Borehole breathing (Ballooning)*.

Borehole ballooning sometimes referred as breathing is an expression used to describe the small volumetric change of the active drilling fluid system, which might occur during drilling operations. The phenomenon of borehole ballooning is caused mainly by following mechanisms [[1],[2]]:

- Thermal expansion and contraction of the drilling fluid.
- Compressibility of the drilling fluid.
- Elastic deformation of the borehole and the cased hole.
- The opening and closing of induced fractures at the near wellbore region.
- The opening and closing of natural fractures intersected during drilling.

By estimating the change in volume of the wellbore caused by one of above mentioned processes, we can avoid confusion with conventional losses or formation kick, consequently nonproductive time (NPT) is reduced.

According to the studies which has been performed by Bjørkevoll et al (1994) and Aadnøy (1996), the volumetric change of an active mud system caused by the elastic deformation of the borehole and the cased hole does not exceed 10% of the total volume

Author α : Phd student, Montanuniversität Leoben (MUL), Department of Petroleum Engineering (DPE), Chair of Drilling and Completion Engineering (CDC), Park -Straße 27, 8700, Leoben, Austria.

Author σ : Head of Petroleum Engineering Department, Montan universität Leoben (MUL), Department of Petroleum Engineering (DPE), Chair of Drilling and Completion Engineering (CDC), Park-Straße 4, 700, Leoben, Austria.

Author ρ : Montan universität Leoben (MUL), Department of Petroleum Engineering (DPE), Chair of rilling and Completion Engineering (CDC), Park-Straße 4, 8700, Leoben, Austria.

Author ω : Universidade Estadual Paulista (UNESP), Faculdade de Engenharia, Câmpus de Guaratinguetá (FEG), Departamento de Mecânica (DME)/PRH48-ANP, Avenida Ariberto Pereira da Cunha 333, Portal das Colinas, 12.516-410 Guaratinguetá, SP, Brazil

Author ¥ : Montanuniversität Leoben (MUL), Department of Petroleum En-gineering (DPE), Chair of rilling and Completion Engineering (CDC), Park-Straße 4, 8700, Leoben, Austria.

variation[3]. Helstrup et al (2001) stated that change in borehole volume due to elastic deformation can be significant and it is mainly driven by wellbore radius, well pressure and Poisson's ratio. Their results show that the change in volume can be as high as 1 bbl for 100 meter depth interval[4]. On 2016 Asad et al performed sensitivity study using syntactic data in order to investigate the effects of different parameters on volumetric deformation of the open borehole, the outcome of the study clearly shows that the volume variation is insignificant and controlled by the drilling fluid weight and temperature[5].

This paper presents standalone software (built on Matlab) to predict and quantify the volumetric change of the active drilling fluid system due to elastic deformation of the open borehole wall, which will assist the drilling engineers to a certain extent to avoid mixing ballooning with other formation flow incidents such as kick or loss. The developed software was designed to fully utilize the existing Geotechnical Mode land rock geo-mechanical properties for any depth interval in order to execute the main objectives of the tool. The

II. BACKGROUND

Recently Elmgerbi et al [5] introduced new analytical equations which are used primarily to predict

the elastic deformation of an open borehole wall, the equations have been validated numerically; this paper presents the recent work of Elmgerbi et al, which is exemplified in standalone software. Generally, the software has multiple features and it is capable to estimate the volumetric change of an open borehole section for different conditions and multi layers by using the Geotechnical Model data such as in situ principal stresses gradients and pore pressure gradient in addition to geo-mechanical properties of the rock like, Poisson's ratio, Young's modulus. The graphical user interface of the software (GUI) has been designed in a manner that allows the user to execute the entire process easily within a short time. The working sequence of the tool consists of five phases, data uploading, data inputting, model selection, final execution and result displaying. Since the graphical analysis is always preferable hence the software generates multiple figures, these figures collectively are comprehensive and readable that leads to valuable analysis. Figure 1 depicts the process roadmap of the developed software.

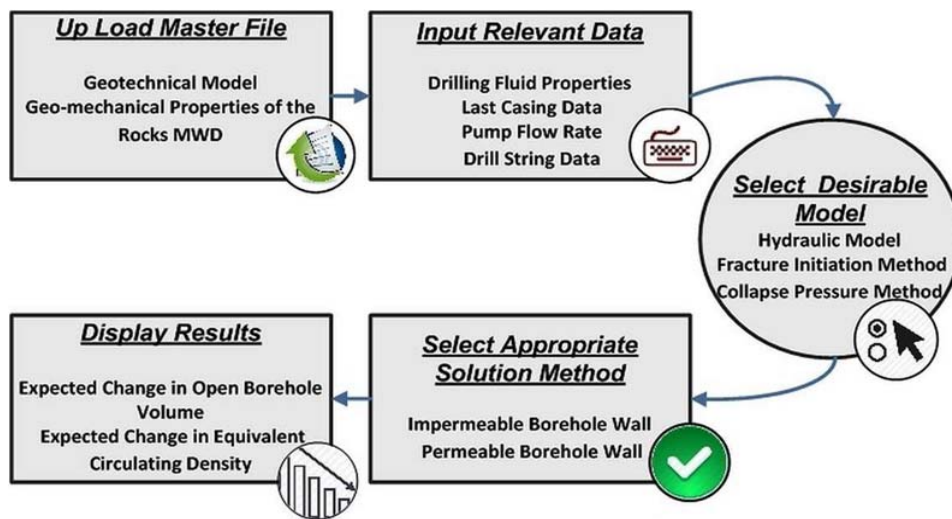


Figure 1: Process Roadmap of the Developed Software.

III. PROCESSING STEPS

a) Data Uploading

Three different data sources are combined in one file (Master file), Geotechnical Model, geo-mechanical properties of the rocks and subsurface data. Therefore it is assumed that the Geotechnical Model and rock properties of the interested field have been already obtained. Building a Geotechnical model can be derived by gathering and analyzing, wire line logs data, down hole measurements data, and drilling

experiences, whereas the rock properties can be determined by combing logs data with laboratory tests [6]. Table 1 shows the essential data categories and sources.

Table 1: Data Categories and Sources

Category	Parameter	Sources
Geotechnical Model	Vertical Principal Stress.	Density and Soniclogs, Cuttings.
	Intermediate Principal Stress.	Image and caliper logs, failure analysis.
	Least Principal Stress.	Leak-off tests, extended leak-off tests, Sonic logs.
	Pore Pressure.	Sonic, resistivity and density logs, seismic data.
Rock Properties	Young's Modulus.	Bulk density log, laboratory core tests, cavings.
	Poisson Ratio.	Bulk density log, laboratory core tests, cavings.
	Biot Constant.	Laboratory core tests.
	Thermal Expansion Coefficient.	Laboratory core tests.
	Cohesive Strength.	Laboratory core tests.
	Friction Angle.	Bulk density log, laboratory core tests.
	Tensile Strength.	Laboratory core tests.
Well Data	Measured Depth.	Rig Data.
	Hole Inclination.	Measuring while drilling.
	Hole Azimuth.	Measuring while drilling.
	Expected Mud Temperature.	Logs.

The Master file, which is recognized by the tool, is a structured text file containing fifteen channels and header information. The header information is located at the beginning of the file and followed by data arrays.

b) *Data Entry*

In the data entry phase the users is allowed to add more information in order to allow effective and successful processing and ensure the integrity of the results. The required data here is particularly related to well, which is under the study.

used by the software. Full mathematical derivations of the entire equations can be found in reference [8].

IV. MATHEMATICAL MODELS AND METHODS

The tool allows the user to choose the desirable hydraulic model and the appropriate failure criteria for both compressive and tensile conditions. Therefore several equations have been integrated with tool. In the next section the utilized equations will be presented.

a) *Hydraulic Models*

The three known hydraulic models, Bingham, Power law and Herschel Bulkley have been integrated with the software in order to make it independent. The main role of the hydraulic model here is to predict the annular pressure loss for the open and cased sections. The table below shows the pressure loss equations



Table 2: Hydraulic Models Equations used by the Developed Software

Model	Flow Regime	Pressure Loss
Bingham	Laminar	$P_l = \frac{PV * v}{1000 * (D_2 - D_1)^2} + \frac{Y_p}{200 * (D_2 - D_1)} \quad (1)$
	Turbulent	$P_l = \frac{\rho^{0.75} * v^{1.75} * PV^{0.25}}{1396 * (D_2 - D_1)^{1.25}} \quad (2)$
Power law	Laminar	$P_l = \left[\frac{144 * v}{D_2 - D_1} * \frac{2 * n + 1}{3 * n} \right]^n * \frac{0.00208 * k}{300 * (D_2 - D_1)} \quad (3)$
	Turbulent	$P_l = \frac{f * \rho * v^2}{21.1 * (D_2 - D_1)} \quad (4)$
Herschel Bulkley	Laminar	$P_l = \left[\frac{0.09984 * k}{14400 * (D_2 - D_1)} \right] * \left[\frac{Y_p}{0.00208 * k} + \left[\left(\frac{192 * (2 * n + 1)}{n * C_a * (D_2 - D_1)} \right) * \left(\frac{0.1016 * Q}{(D_2^2 - D_1^2)} \right) \right]^n \right] \quad (5)$
	Turbulent	$P_l = \frac{7.48 * f * (0.002217 * Q)^2 * \rho}{0.005712 * (D_2 - D_1) * (D_2^2 - D_1^2)^2} \quad (6)$

b) Fracture Initiation Pressure and Collapse Pressure Methods

In case the Geotechnical Model does not include fracture initiation pressure and collapse

pressure, the software offers several methods, which can be used to predict upper and lower bounds of the safe mud pressure window.

Table 3: Fracture Initiation Pressure Equations used by the Developed Software

per Boundary [Fracture Initiation Pressure] Methods[9][10], [11], [12]	
Method	Fracture Initiation Pressure
Hubbert & Willis	$P_f = \frac{(1 - \sin(\phi))}{(1 + \sin(\phi))} (\sigma_v - (\alpha * P_p)) + (\alpha * P_p) \quad (7)$
Eaton	$P_f = \frac{v}{(1 - v)} (\sigma_v - (\alpha * P_p)) + (\alpha * P_p) \quad (8)$
Minimum Stress	$P_f = \sigma_h \quad (9)$
Bellotti & Giacca	$P_f = \frac{2 * v}{(1 - v)} (\sigma_v - (\alpha * P_p)) + (\alpha * P_p) \quad (10)$
Hoop Stress Method	$P_f = 3\sigma_h - \sigma_H - (\alpha * P_p) + \sigma_t^{\Delta t} + T \quad (11)$

Table 4: Collapse Pressure Equations used by the Developed Software

Lower Boundary [Collapse Pressure] Methods[13], [14]	
Mohr Coulomb	
Case#1	$p_{wc} = \frac{(3\sigma_H - \sigma_h + \sigma_t^{\Delta t}) * (1 - \sin(\phi))}{2} - S_o * \cos(\phi) + (\alpha * P_p) * \sin(\phi) \quad (12)$
Case#2	$p_{wc} = \frac{1}{(1 + \sin(\phi))} * [(\sigma_v + \sigma_t^{\Delta t} + 2 * v(\sigma_H - \sigma_h)) * (1 - \sin(\phi)) - 2 * S_o * \cos(\phi) + (\alpha * P_p) * \sin(\phi)] \quad (13)$
Modified Lade	
	$I_3 = \frac{I_1^3}{(27 + \eta)} \quad (14)$

The detailed steps for deriving the equations can be found in Appendix

c) *Stress Transformation Equations*

In case the borehole is horizontal or inclined, the stress transformation equations are triggered in order to transform the stresses to a new Cartesian

coordinate system, where two stresses are perpendicular to the borehole whereas the third stress is parallel to the axes of the borehole[15].

Table 5: Stress Transformation Equations Used by the Developed Software

Stress Transformation Equations	
$\sigma_H^\circ = (\sigma_H * (\cos(\omega))^2 + \sigma_h * (\sin(\omega))^2) * (\cos(\delta))^2 + \sigma_v * (\sin(\delta))^2$	(15)
$\sigma_h^\circ = (\sigma_H * (\sin(\omega))^2 + \sigma_h * (\cos(\omega))^2)$	(16)
$\sigma_v^\circ = (\sigma_H * (\cos(\omega))^2 + \sigma_h * (\sin(\omega))^2) * (\sin(\delta))^2 + \sigma_v * (\cos(\delta))^2$	(17)
$\tau_{xy}^\circ = \frac{1}{2}(\sigma_H - \sigma_h) * (\sin(2\omega)) * (\cos(\delta))$	(18)
$\tau_{xz}^\circ = \frac{1}{2}(\sigma_H * (\cos(\omega))^2 + \sigma_h * (\sin(\omega))^2 - \sigma_v) * (\sin(2\delta))$	(19)

d) *True Vertical Depth Determination Method*

There are several known methods of computing true vertical depth, one of these methods is the

minimum curvature, it is theoretically the most accurate and most commonly used, hence it was integrated with software[16].

Table 6: Minimum Curvature Method Equations Used by the Developed Software

Minimum Curvature Method	
$DL = \cos^{-1} * [\sin(\delta_1) * \sin(\delta_2) * \cos(\omega_2 - \omega_1) + \cos(\delta_1) * \cos(\delta_2)]$	(20)
$RF = \tan\left(\frac{DL}{2}\right) * \frac{180}{\pi} * \frac{2}{DL}$	(21)
$\Delta TVD = [\cos(\delta_1) + \cos(\delta_2)] * \left[\frac{RF * \Delta MD}{2}\right]$	(22)

e) *Solution Methods*

Two solution methods are available, one is for impermeable borehole wall whereas the second for permeable. Practically, the impermeable proposed solution is valid once the rock formation is exposed to the drilling fluid and last as long as no filtration occurs

[Initial condition], whereas the permeable solution is effective only when a stable mud cake is built [Steady stat condition]. Only the final formula of the two methods will be mentioned here. Therefore for more details refer to reference [5].

Table 7 : Radial Elastic Displacement Equations Used by the Developed Software

Radial Elastic Displacement	
Permeable	$u = r * \frac{1}{E} \left[P_w * (1 + \nu) - (\alpha * P_w) * (2\nu - 1) - (1 - \nu) * (\sigma_t^{\Delta t} + 2\eta (P_w - (\alpha * P_p))) \right] - (\nu^2 - 1) * (2(\sigma_H - \sigma_h) \cos(2\theta) + 4 * \tau_{xy} * \sin(2\theta)) - \sigma_H - \sigma_h + \nu * \sigma_v$ (23)
Impermeable	$u = r * \frac{(1 + \nu)}{E} \left[P_w - \frac{(2\nu - 1)}{(1 + \nu)} * (\alpha * P_p) - \frac{(1 - \nu)}{(1 + \nu)} * \sigma_t^{\Delta t} - \frac{1}{(1 + \nu)} * (\sigma_H + \sigma_h - \nu * \sigma_v) - 2 * (\nu - 1) * ((\sigma_H - \sigma_h) \cos(2\theta) + 2 * \tau_{xy} * \sin(2\theta)) \right]$ (24)

V. DELIVERABLES OF THE SOFTWARE

Several figures are generated, which would assist to improve individual analysis quality and provide a simple visual way of analyzing. The following points show the main figures that displayed by the developed software:

- Well profile.
- Safe mud pressure window.
- Volumetric change of the open borehole section.
- Change in the Equivalent Circulating Density (ECD).
- Open borehole section condition.

VI. INTERNAL WORKFLOW DESCRIPTION

Sequential steps are performed at the back ground of the software in order to achieve the main objectives of the software. Figure 2 below depicts these steps. As it is illustrated in Figure 2, the process starts by computing the annular pressure loss between the casing and drill string, here the given casing depth and drill string geometry are used. Then the software starts fetching the data point from the master file, one by one, each time several steps are performed, the steps are repeated for each single data point till the last data point. Eventually the cumulative volumetric change of the open borehole section and the change in Equivalent Circulating Density (ECD) are computed and graphically displayed for different flow rates. The change in (ECD) referred to here is the difference between the theoretical (ECD) [Calculated based on the original shape of the open borehole section] and predicted (ECD) [Calculated based on deformed shape of the open borehole section].



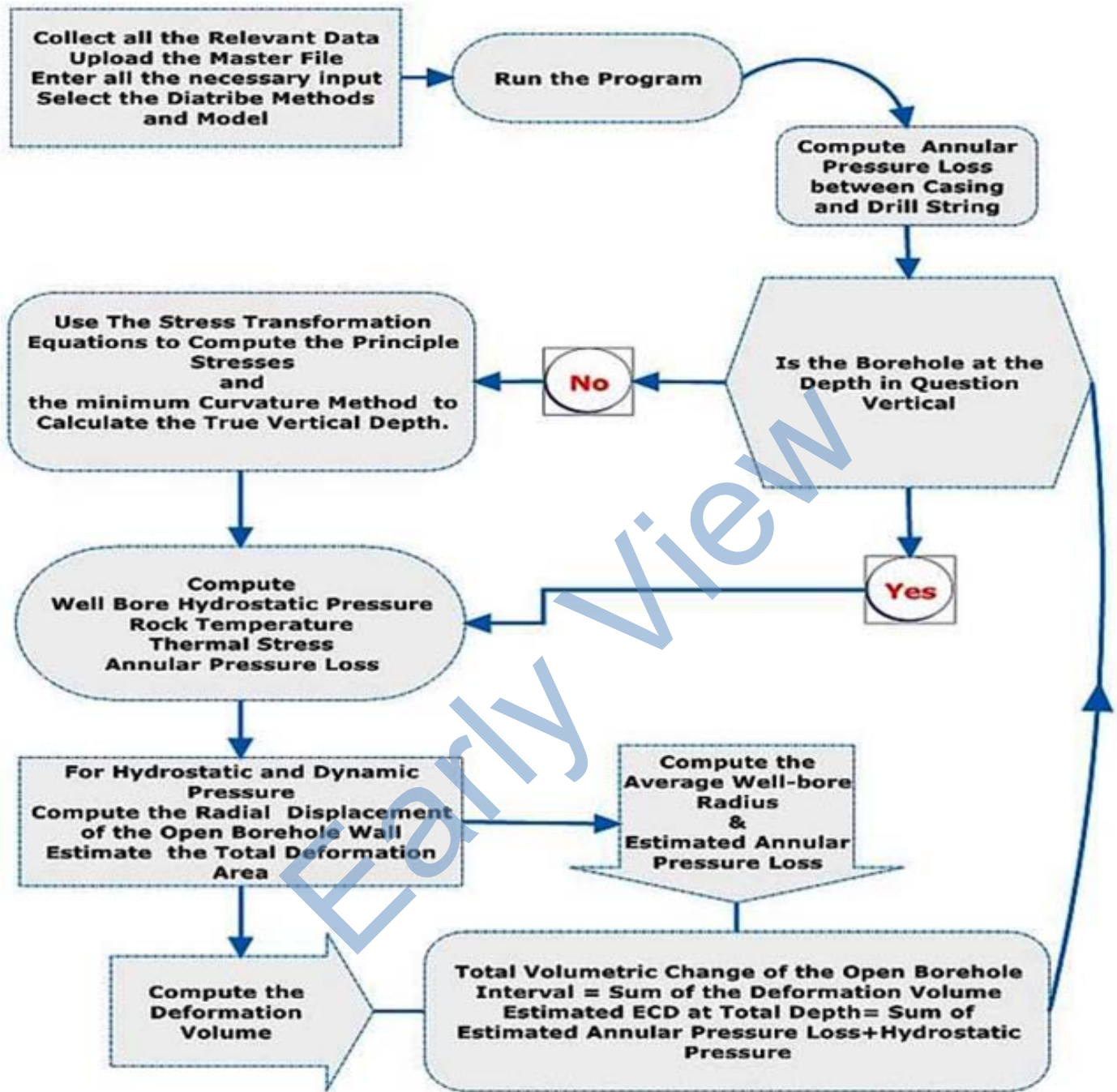


Figure 2 : Internal Workflow of the Developed Software

VII. CASE STUDY

Necessary analysis for the presented case study performed using historical data belonging to two wells. The main objectives of the study were to measure the effects of different controllable and uncontrollable parameters on the volumetric changes of the open borehole section and to evaluate any expected changes which would occur to ECD saccordingly. The initial well condition for the example mentioned can be seen in Table 8.

Table 8: Well Characteristics and the Relevant Data used for the Study

	Well A	Well B
Last Casing Size and Depth [ft]	9 5/8" - 12600	7 5/8" - 16500
Well Type	Vertical	Slightly Deviated
Total Measured Depth [ft]	13400	19050
Open Hole Section Thickness [ft] and Size [in]	800 - 8 1/2"	2550 - 6 1/2"
Mud Weight [ppg]	10	11.5
Hydraulic Model Used	Bingham	Herschel Bulkey
Fracture Initiation Pressure Method Used	Eaton	Bellotti & Giacca
Collapse Pressure Method Used	Modified Lade	Mohr Coulomb
Drill Pipe length [ft] and Size [in]	12800 - 4 1/2"	17500 - 3 1/2"
Heavy Weight Drill Pipe length [ft] and Size [in]	200 - 5"	800 - 3 1/2"
Drill Collar length [ft] and Size [in]	400 - 5 1/2"	750 - 4 3/4"
Initial Flow Rate [gpm]	500	700
Viscometer Reading [600-300-6-3] [1/sec ⁻¹]	26-20-8-6	38-26-6-5

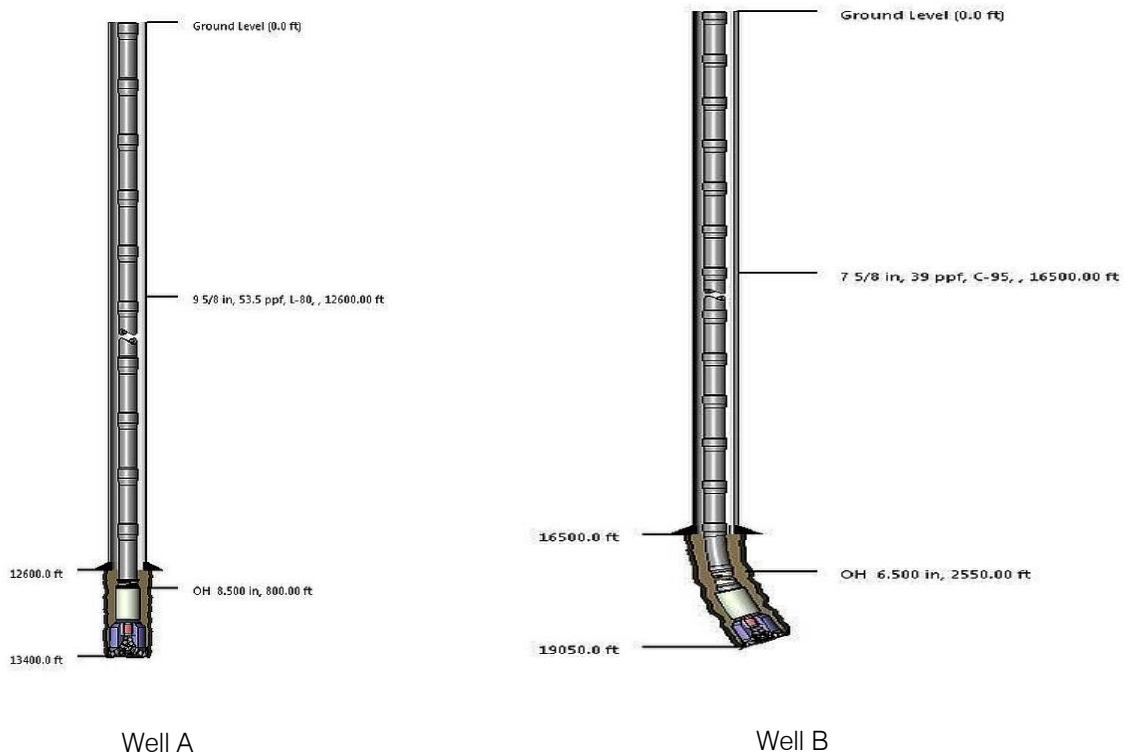


Figure 3 : Wellbore Schematic

Three different scenarios have been studied as following:

- In first scenario, the initial well condition was applied (Table 8).
- In the second scenario, the effect of the mud weight was investigated.
- In the third scenario, the influence of drilling fluid temperature was studied.

In each scenario the pump flow rate was gradually increased from the initial rate to maximum allowable rate.

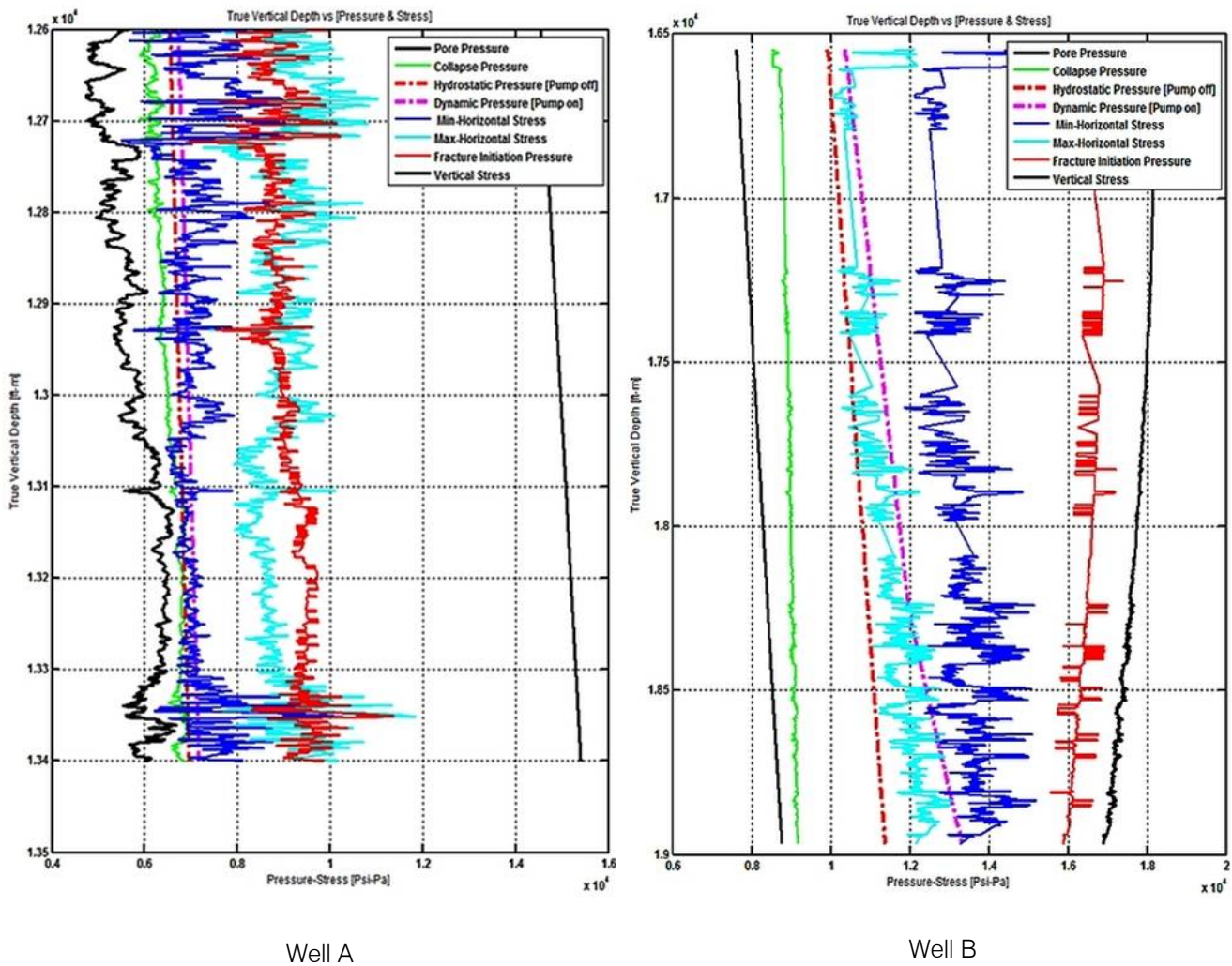


Figure 4: Safe Mud Pressure Window

a) Well A

As it is clearly indicated in Figure 4, this well can be characterized as the one with narrower safe mud pressure window consequently the maximum permissible pump flow rate was limited to 1000 gpm. Figure 5 depicts the results of the studied scenarios. In general, the volumetric change of the open borehole section and change in ECD increase with increasing the pump flow rate. However the changes are not significant and they can be ignored. Although in second scenario the mud weight was higher, it did not make remarkable changes, the reason for that mainly related to the contraction and expansion of the open borehole, in all scenarios, the borehole was always in contraction status even with higher flow rate [Figure 6].

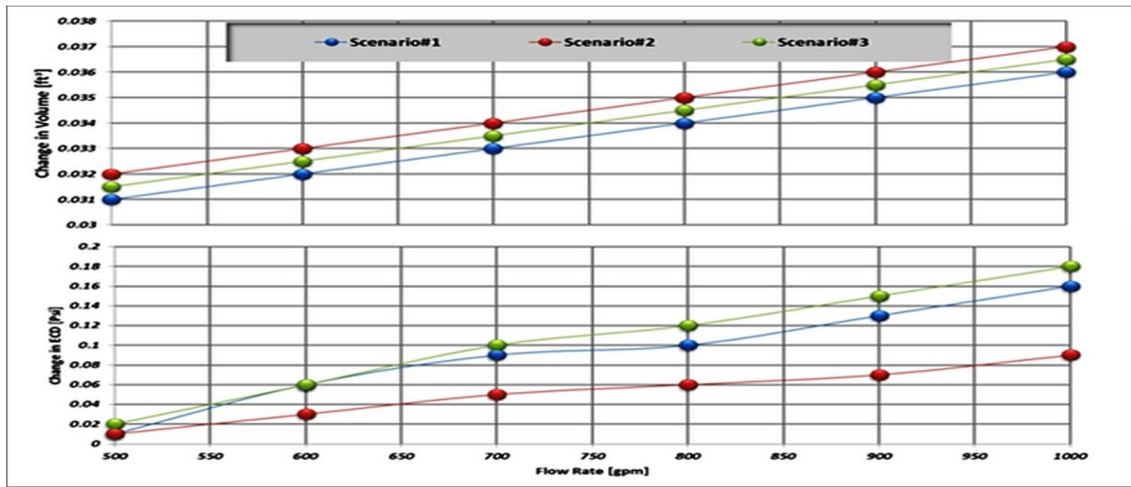


Figure 5: Expected Change in Open Borehole Volume and ECD for Different Pump Flow Rate [Well A]

[In the second scenario the mud weight was increased to 10.5 ppg instead of 10 ppg, while in third scenario, the drilling fluid temperature is assumed to be 127°C for the entire open hole section and 0.925 [°C/100ft] used as thermal gradient]

The results show another important observation that the change in ECD in second scenario is always less comparing to the other scenarios, again the main reason of that is the borehole condition. Increasing mud weight would intend to change the borehole from contraction condition to expansion condition, hence the average radius of the deformation borehole increases and the cumulative annular pressure loss at the bottom

of the borehole decreases accordingly. Comparing the third scenario with first scenario, slight increase in the volumetric change of the open borehole section can be noted, it is caused mainly by the thermal stress. The existence of the thermal stress will cause the drill-induced stresses to increase, consequently the open borehole shrinks and the annular pressure loss increases. Therefore, higher dynamic wellbore pressure is expected, it cause the open borehole section to expand, due to this expansion, the difference in deformation volume between the pump on and off is higher.

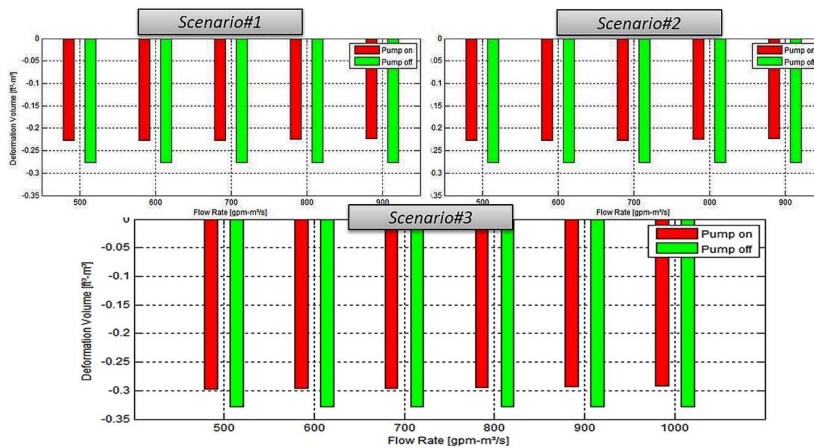


Figure 6 : Cumulative Deformation Volume of the Open borehole section for Different Pump Flow Rate [Well A]

[The red bar shows the borehole condition under static status [pump off], whereas the green bar illustrates the borehole condition under dynamic status [pump on]. the negative number indicates that the borehole is under contraction condition]

b) Well B

This well has wider safe mud pressure window, which makes it a good example to study the impact of the borehole condition in term of contraction and expansion on volumetric change of the open borehole

and change in ECD. Three important observations can be extracted from the 3 scenarios are;

- The volumetric change of the open borehole and change in ECD increase constantly with pump flow rate.
- In the second scenario, the borehole condition changes from contraction status to expansion status, consequently the volumetric change is higher and the change in ECD is lower comparing to the first scenario. The change in ECD in this case is

negative, in other words, the predicted ECD at the bottom of the hole is less than the theoretical ECD.

- The slight increase in volumetric change and the change in ECD in the third scenario are due to the thermal stress effect.

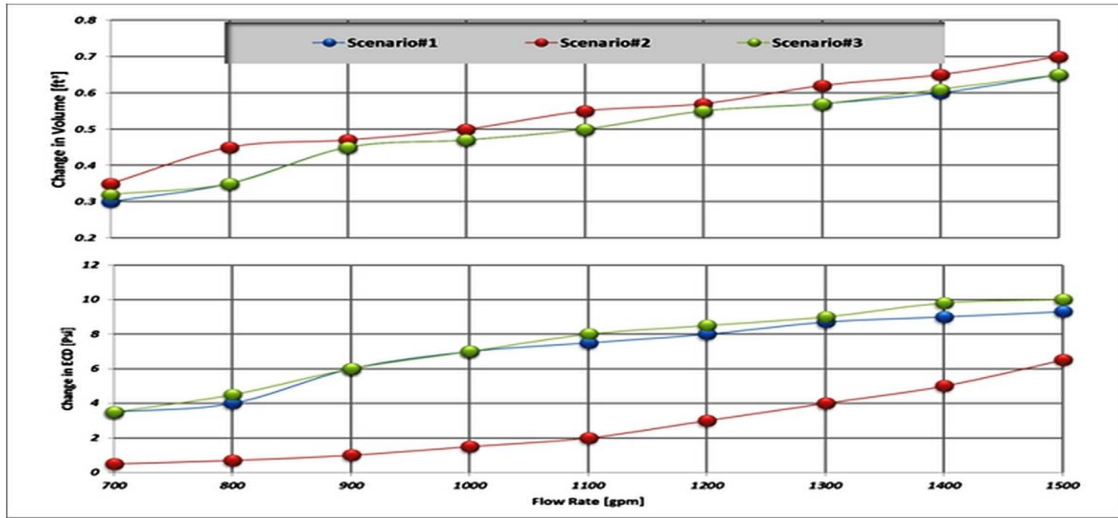


Figure 7: Expected Change in Open Borehole Volume and ECD for Different Pump Flow Rate [Well B]

[In the second scenario the mud weight was increased to 13.5 ppg instead of 11.5 ppg, while in third scenario, the drilling fluid temperature is assumed to be

177°C for the entire open hole section and 0.925 [°C/100ft] used as thermal gradient]

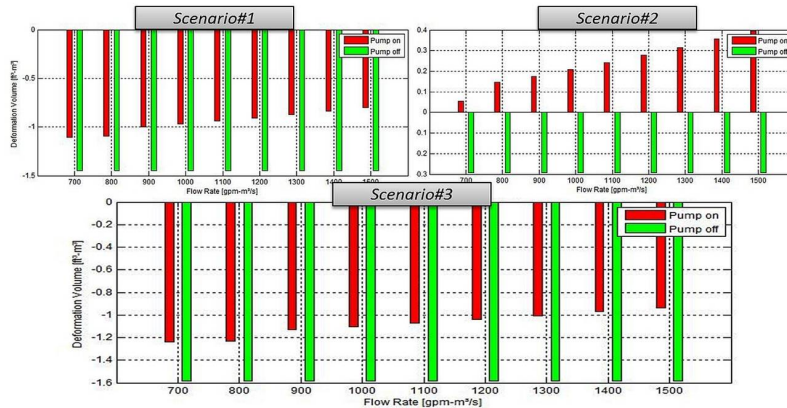


Figure 8: Cumulative Deformation Volume of the Open Borehole Section for Different Pump Flow Rate [Well B]

[It is obvious that the open borehole is under contraction status in first and third scenario, in contrast it is under expansion status in the second scenario.]

VIII. CONCLUSION

The main conclusion of the presented work can be summarized in the following points:

- For the purpose of accurately quantifying the volumetric change of an open borehole section and its impact on the hydraulic system, Standalone software has been developed, it has multiple features and it is able to estimate the volumetric change of an open borehole section and to predict any possible change might occur to the ECD for any

given well by utilizing the Geotechnical Model data, geo-mechanical properties of the rocks and subsurface data.

- Detailed description for all the equations and models of the developed software have been provided.
- Since the graphical analysis is always preferable hence the developed software generates multiple charts, these charts collectively are comprehensive and readable that leads to valuable analysis.
- The findings of two case studies can be concluded as following:
 - The elastic deformation of an open borehole section wall certainly occurs and its severity

depends on geotechnical properties of encountered formation, magnitude of the in situ principle stresses, induced stresses, well geometry, well profile and the operational margin between dynamic and the hydrostatic pressure.

- o The volumetric change of the open borehole section and change in ECD increase with increasing the pump flow rate.
- o The static condition [pump off] of an open borehole section in terms of contraction and expansion is mainly driven by the status of the in situ principal stresses and the drilling fluid weight.
- o The changing magnitude of ECD depends mainly on the open borehole static [Pump off] condition, if the borehole is under contraction status when the pump is off, two cases could exist once the pump is started:
 - The borehole could continue to be under contraction status; in this case the change in ECD will be positive [the predicted ECD will be higher than the theoretical ECD].
 - The second possible situation occurs if the open borehole condition changes from contraction to expansion, in this case the predicted ECD will be less than the theoretical ECD and consequently the change in ECD will be negative.

REFERENCES RÉFÉRENCES REFERENCIAS

1. Lavrov, A. and Tronvoll, J. 2005. Mechanics of Borehole Ballooning in Naturally-Fractured Formations. Presented at the SPE Middle East Oil & Gas Show and Conference, Bahrain, 12-15 March 2005. SPE-93747-MS. <http://dx.doi.org/10.2118/93747-MS>.
2. Eirik, K. and Aadnøy, S. Temperature Model Provides Information for Well Control. Oil & Gas Journal, September 1998. <http://www.ogj.com/articles/print/volume-96/issue-37/in-this-issue/drilling/temperature>
3. Aadnøy, S. and Brent, S. 2010. Evaluation of ballooning in deep wells. In Modern Well Design, second edition, Appendix B, 294. London, UK: Taylor & Francis Group.
4. Helstrup, A. Rahman, M.K. Hossain, M.M. and Rahman, S. 2001. A Practical Method for Evaluating Effects of Fracture Charging and/or Ballooning When Drilling High Pressure, High Temperature (HPHT) Wells. Presented at SPE/IADC Drilling Conference, Netherlands, Amsterdam, 27 February-1 March 2001. SPE-67780-MS. <http://dx.doi.org/10.2118/67780-MS>.
5. Elmgerbi, A. Thonhauser, G. Prohaska, M. et al. General Analytical Solution for Estimating the Elastic Deformation of an Open Borehole Wall. International Journal of Scientific & Engineering Research, Volume 7, Issue 1, 13 pages, January 2016. <http://www.ijser.org/onlineResearchPaperViewer.aspx?General-Analytical-Solution-for-Estimating-the-Elastic-Deformation-of-an-Open-Borehole-Wall.pdf>.
6. Al-Maamori, H. El Naggar, M. and Micic, S. A Compilation of the Geo-Mechanical Properties of Rocks in Southern Ontario and the Neighbouring Regions. Open Journal of Geology, Volume 4, 19 pages, April 2014. dx.doi.org/10.4236/ojg.2014.45017.
7. Akbar Ali, A. Brown, T. Delgado, R. et al. Watching Rocks Change—Mechanical Earth Modeling. Oilfield Review, 2013. https://www.slb.com/~media/Files/resources/oilfield.../p22_39.pdf.
8. Guo, B. and Liu, G. 2011. Mud Hydraulic Fundamentals. In Applied Drilling Circulation System, first edition, Chapter 2, 19-57: Gulf Professional Publishing is an imprint of Elsevier.
9. Hubbert, M. K. and Willis, D. G., Mechanics of Hydraulic Fracturing. AIME Petroleum Transactions, Vol. 210, 1957, pp. 153-168. <https://www.depts.ttu.edu.../Hubbert%20and%20Willis,%201972%20me>.
10. Ben A, E.. Fracture Gradient Prediction and Its Application in Oilfield Operations. Journal of Petroleum Technology, Volume 21, Issue 10, 8 pages, October 1969. <http://dx.doi.org/10.2118/2163-PA>.
11. Peng, S. and Zhang, J. 2007. Wellbore/borehole stability. In Engineering Geology for underground Rocks, first edition, Chapter 7, 177. Berlin, Germany: Springer Science and Business Media.
12. Bellotti, P. and Giacca, D. Pressure evaluation improves drilling performance. Oil and Gas Journal, Sept. 11, 1978.
13. Bernt, S. and Aadnøy, U. Bounds on In-Situ Stress Magnitudes Improve Wellbore Stability Analyses. Journal of Petroleum Technology, Volume 10, Issue 2, 6 pages, June 2005. <http://dx.doi.org/10.2118/87223-PA>.
14. Ewy, R. Wellbore-Stability Predictions by Use of a Modified Lade Criterion. Journal of Petroleum Technology, Volume 14, Issue 2, 7 pages, June 1999. <http://dx.doi.org/10.2118/56862-PA>.
15. Aadnøy, S. and Looyeh, R. 2011. Stresses Around A Wellbore. In Petroleum Rock Mechanics Drilling Operations And Well Design, first edition, Chapter 10, 157: Gulf Professional Publishing is an imprint of Elsevier.
16. Sawaryn, S. and Thorogood, J. 2003. A Compendium of Directional Calculations Based on the Minimum Curvature Method. Presented at the SPE Annual Technical Conference and Exhibition, Denver, Colorado, U.S.A., 5 – 8 October 2003. SPE-84246. <http://dx.doi.org/10.2118/84246-MS>.

NOMENCLATURE

P_l	Pressure Loss [Psi/ft, Pa/m]
ρ	Density [ppg]
PV	Plastic viscosity [cP]
v	Mean velocity [Ft/second]
Y_p	Yield point [lb/100ft ²]
D_1	Drill string outer diameter [in, m]
D_2	Casing inner diameter, open hole diameter [in, m]
n	Behavior Index [Dimensionless]
k	Consistency Index [EqcP]
f	Friction Factor [Dimensionless]
C_a	Herschel Bulkley variable [Dimensionless]
Q	Flow rate [gpm, m ³ /second]
P_f	Fracture initiation pressure [Psi,Pa]
ϕ	Rock friction angle [°]
σ_v	Vertical principle stress [Psi,Pa]
α	Biot's elastic constant [Dimensionless]
P_p	Formation pore pressure [Psi,Pa]
ν	Poisson ratio [Dimensionless]
σ_h	Minimum horizontal principle stress [Psi,Pa]
σ_H	Maximum horizontal principle stress [Psi,Pa]
$\sigma_t^{\Delta t}$	Thermal stress [Psi,Pa]
T	Rock tensile strength [Psi,Pa]
p_{wc}	Collapse pressure [Psi,Pa]
S_o	Rock cohesive strength [Psi,Pa]
I_1	First stress invariant [Psi,Pa]
I_3	Third stress invariant [Psi ³ ,Pa ³]
η	Material parameter related to friction [Dimensionless]
σ_{11}	Major effective principal stress [Psi,Pa]
σ_{22}	Intermediate effective principal stress [Psi,Pa]
σ_{33}	Minor effective principal stress [Psi,Pa]
σ_{rr}	Effective radial stress
$\sigma_{\theta\theta}$	Effective tangential stress
σ_{zz}	Effective stress along the borehole axis
θ	Angle around the borehole measured anticlockwise from the azimuth of σ_H
$\tau_{\theta z}$	Shear stress in $[\theta, z]$ plane [Psi,Pa]
τ_{xz}	Shear stresses in $[x, z]$ plane [Psi,Pa]
τ_{xy}	Shear stresses in $[x, y]$ plane [Psi,Pa]
τ_{yz}	Shear stresses in $[y, z]$ plane [Psi,Pa]
S_1	Material parameter [Psi,Pa]
u	Radial elastic displacement for the borehole [in, m]
r	Wellbore radius [in, m]
E	Young's modulus [Psi,Pa]
η	Poroelastic stress coefficient [Dimensionless]
P_w	Borehole Pressure [Psi,Pa]
σ_H°	Transformed maximum horizontal stress [Psi,Pa]
σ_h°	Transformed minimum horizontal stress [Psi,Pa]
σ_v°	Transformed vertical stress [Psi,Pa]
τ_{xy}°	Transformed shear stresses in $[x, y]$ plane [Psi,Pa]
τ_{xz}°	Transformed shear stresses in $[x, z]$ plane [Psi,Pa]
ω	Borehole azimuth [°]
δ	Borehole inclination [°]
DL	Dogleg severity [°]
RF	Ratio factor [Dimensionless]
ΔTVD	Change in true vertical depth [ft,m]
ΔMD	Change in measured depth [ft,m]

APPENDIX

Mohr Coulomb

General failure Equation is;

$$\sigma_{11} - \sigma_{33} = 2 * S_o * \text{COS}(\phi) + (\sigma_{11} + \sigma_{33}) * \text{SIN}(\phi) \text{ (A1)}$$

Well bore collapse is expected to occur at the azimuth of σ_h , in other word at $\theta=90^0$, hence the induced stresses can be calculated using the following equations;

$$\sigma_{rr} = P_{wc} - (\alpha * P_p) \text{ (A2)}$$

$$\sigma_{\theta\theta} = 3\sigma_H - \sigma_h - P_{wc} - (\alpha * P_p) + \sigma_t^{\Delta} \text{ (A3)}$$

$$\sigma_{zz} = \sigma_v - (\alpha * P_p) + \sigma_t^{\Delta} + 2 * \nu(\sigma_H - \sigma_h) \text{ (A4)}$$

$$\tau_{\theta z} = 2 * (-\tau_{xz}) \text{ (A5)}$$

Since P_{wc} is unknown for comparison it is assumed that $P_{wc} = P_p$

Case#1

$$\sigma_{rr} \leq \sigma_{zz} \leq \sigma_{\theta\theta} \text{ Therefore}$$

In Equation A1

$$\sigma_{11} = \sigma_{\theta\theta} \text{ and } \sigma_{33} = \sigma_{rr}$$

Insert EqA2 and A3 into Eq A1, after few mathematical steps and arrangements we end up with the following Equation for collapse pressure:

$$P_{wc} = \frac{(3\sigma_H - \sigma_h + \sigma_t^{\Delta}) * (1 - \text{SIN}(\phi))}{2} - S_o * \text{COS}(\phi) + (\alpha * P_p) * \text{SIN}(\phi) \text{ (A6)}$$

Case#2

In case two the following condition is assumed

$$\sigma_{rr} \leq \sigma_{\theta\theta} \leq \sigma_{zz}$$

Therefore in Eq A1

$$\sigma_{11} = \sigma_{zz} \text{ and } \sigma_{33} = \sigma_{rr}$$

Now by inserting A2 and A4 into Eq A1 collapse pressure for the second case can be derived:

$$P_{wc} = \frac{1}{(1 + \text{SIN}(\phi))} * [(\sigma_v + \sigma_t^{\Delta} + 2 * \nu(\sigma_H - \sigma_h)) * (1 - \text{SIN}(\phi)) - 2 * S_o * \text{COS}(\phi) + (\alpha * P_p) * \text{SIN}(\phi)] \text{ (A7)}$$

Modified Lade

$$\frac{I_1^3}{I_3} = 27 + \text{ (A8)}$$

$$I_1 = (\sigma_{11} + S_1) + (\sigma_{22} + S_1) + (\sigma_{33} + S_1) \text{ (A9)}$$

$$I_3 = (\sigma_{11} + S_1) * (\sigma_{22} + S_1) * (\sigma_{33} + S_1) + 2 * \tau_{xy} * \tau_{xz} * \tau_{yz} - (\sigma_{11} + S_1)\tau_{yz}^2 - (\sigma_{22} + S_1)\tau_{zx}^2 - (\sigma_{33} + S_1)\tau_{xy} \text{ (A10)}$$

$$S_1 = \frac{S_o}{\text{TAN}(\phi)} \text{ (A11)}$$

$$\eta = \frac{4 * (\text{TAN}(\phi))^2 * (9 - 7 * \text{SIN}(\phi))}{(1 - \text{SIN}(\phi))} \text{ (A12)}$$

Because the collapse occurs at $\theta=90^0$, Eq A9 and A10 for cylindrical coordinate will have the following form:

$$I_1 = (\sigma_{rr} + S_1) + (\sigma_{\theta\theta} + S_1) + (\sigma_{zz} + S_1) \text{ (A13)}$$

$$I_3 = (\sigma_{rr} + S_1) * (\sigma_{\theta\theta} + S_1) * (\sigma_{zz} + S_1) - (\sigma_{rr} + S_1)\tau_{\theta z} \text{ (A14)}$$

By substituting σ_{rr} , $\sigma_{\theta\theta}$, σ_{zz} and $\tau_{\theta z}$ in Eq A13 and A14 with Eq A2, A3, A4 and A5 respectively

$$I_1 = \sigma_v - 3 * (\alpha * P_p) + 2 * \sigma_t^{\Delta} + 3 * S_1 + \sigma_H * (2\nu + 3) - \sigma_h * (2\nu + 1) \text{ (A15)}$$

$$I_3 = (P_{wc} - (\alpha * P_p) + S_1) * (3\sigma_H - \sigma_h - P_{wc} - (\alpha * P_p) + \sigma_t^{\Delta t} + S_1) * (\sigma_v - (\alpha * P_p) + \sigma_t^{\Delta t} + 2\nu(\sigma_H - \sigma_h) + S_1) - (P_{wc} - (\alpha * P_p) + S_1) * (4 * \tau_{xz}^2) \quad (A16)$$

Now back to Eq A8 rearrange it

$$I_3 = \frac{I_1^3}{(27 + \eta)}$$

Finally replace I_1 , I_3 , S_1 and η with Eq A15, A16, A11 and A12 respectively in Eq A8, the right side of Eq A8 is independent of P_{wc} , while the left side is a quadratic expression in P_{wc} . Therefore by solving Eq A8 the collapse pressure P_{wc} can be obtained. Since two solutions are expected, the collapse pressure equals the lesser one.



This page is intentionally left blank